On the Stability of the Mean-Field Spin Glass Broken Phase under Non-Hamiltonian Perturbations*

G. Iori[(a)] and E. Marinari[(b)]

(a): Dipartimento di Fisica and Infn, Università di Roma *La Sapienza*

P. A. Moro 2, 00185 Roma (Italy)

(b): Dipartimento di Fisica and Infn, Università di Cagliari

Via Ospedale 72, 09100 Cagliari (Italy)

`iorig@roma1.infn.it`

`marinari@ca.infn.it`

November 27, 1996

Abstract

We study the dynamics of the SK model modified by a small non-hamiltonian perturbation. We study aging, and we find that on the time scales investigated by our numerical simulations it survives a small perturbation (and is destroyed by a large one). If we assume we are observing a transient behavior the scaling of correlation times versus the asymmetry strength is not compatible with the one expected for the spherical model. We discuss the slow power law decay of observable quantities to equilibrium, and we show that for small perturbations power like decay is preserved. We also discuss the asymptotically large time region on small lattices.

`cond-mat/yymmnnn`

*In memory of our friend Giovanni Paladin.

1 Introduction

The non hamiltonian generalization of the dynamic of the SK model is an interesting problem. The main question is if a complex dynamic (implying aging, slow power like decays and related effects) is stable under a small non hamiltonian perturbation.

The problem has been analyzed in detail in many papers, but definite conclusions are difficult to reach. Crisanti and Sompolinsky [1, 2] have studied a simplified version of the mean field, the spherical model (see later in the text), and have shown that for this model a small perturbation is enough do destabilize the glassy phase. For large asymmetry two other studies agree with this conclusion [3, 4].

The fully asymmetric model has been studied in detail in [1, 4, 5, 6]. The $T = 0$ case has been discussed in [7, 8, 9, 10]. Techniques like damage spreading have been also used [11] (by reaching conclusions about the possible survival of a complex behavior similar to the ones we reach here). Also recently the p-spin model (with $p > 2$) has been studied [12].

Here we will try to distinguish about two different aspects of the non hamiltonian generalization of the SK model. On the one side we will discuss its dynamical behavior, by focusing on aging like effects. On the other side we will look at the long time *equilibrium* limit of the model, on smaller lattices.

In section (2) we remind to the reader some of the theoretical results. In section (3) we give the definitions we will need in the following. In section (4) we discuss aging-like effects. In section (5) we show slow, power law decays. These two sections deal with dynamic behaviors: we use large lattices and we stay far from equilibrium. In section (6) we discuss long equilibrium runs, on small lattices. In section (7) we draw our conclusions.

2 Theory

Even if, as we have said, a large amount of work has been devoted to the study of non hamiltonian disordered models [1] – [12], the main results about the general case of the finite T spherical spin model with non-symmetric couplings have been obtained in [1], while many of the other works deal with special cases like the $T = 0$ dynamics or the fully asymmetric case. Here we are interested to the finite T dynamics of a SK model (as opposed to the spherical model) that is perturbed by a small, non hamiltonian term, and as we will discuss now not much is known about this case.

In order to make the situation clearer let us give to the reader at least a sketchy idea about the results obtained in [1, 2], that are based on the dynamic mean field formalism of [13].

The generalization of the usual spin glass dynamic is done by using the couplings

$$J_{i,j} = J^S_{i,j} + kJ^{AS}_{i,j} \;, \tag{1}$$

where $J^S_{i,j} = J^S_{j,i}$, and $J^{AS}_{i,j} = -J^{AS}_{j,i}$ (with a definition of the asymmetry parameter k slightly different from the ϵ we will use in the following, see (17)). Both J types have zero average over the disorder and

$$\overline{J^{S^2}} = \overline{J^{AS^2}} = \frac{J^2}{N}\,\frac{1}{1+k^2} \;, \tag{2}$$

where by the overline we indicate the average over the disorder and by the brackets we denote the thermal average. At first one writes the non hamiltonian generalization of the *soft spin* ($\sigma_i \in [-\infty, +\infty]$) SK mean field model, whose dynamics is governed by the Langevin equation

$$\Gamma_0^{-1} \frac{\partial}{\partial t}\sigma_i(t) = -r_0\sigma_i(t) - \frac{\delta V(\sigma_i(t))}{\delta\sigma_i(t)} + \sum_j J_{i,j}\sigma_j(t) + h_i(t) + \xi_i(t) \;, \tag{3}$$

where J contains the two contributions of (1). The potential controls fluctuations in the amplitude of the soft spins $\sigma_i(t)$, h is a local external field, and ξ is a white noise, with

$$\langle \xi_i(t)\xi_j(t')\rangle = \frac{2T}{\Gamma_0}\delta(t-t')\delta_{i,j} \;. \tag{4}$$

T is the equivalent of a temperature (for this model, where a priori one cannot expect to reach thermal equilibrium). The autocorrelation

$$C(t) = \overline{\langle \sigma_i(t+t')\sigma_i(t')\rangle} \;, \tag{5}$$

and the response function

$$\frac{\delta\overline{\langle\sigma_i(t+t')\rangle}}{\delta h_i(t')}\Big|_{h=0} \;, t \geq 0 \;, \tag{6}$$

are the main dynamical observable quantities. The static susceptibility χ is defined as

$$\chi \equiv \int_{-\infty}^{+\infty} dt\; G(t) \;. \tag{7}$$

After taking the $N \to \infty$ limit one can use the approach of [13] and write the mean field equations of motion

$$\Gamma_0^{-1}\frac{\partial}{\partial t}\sigma_i(t) = \; - \; r_0\sigma_i(t) - \frac{\delta V(\sigma_i(t))}{\delta\sigma_i(t)} + h_i(t) + \phi_i(t)$$
$$+ \; J^2\frac{1-k^2}{1+k^2}\int_{-\infty}^{t} dt' \; G(t-t') \; \sigma_i(t') \; , \tag{8}$$

where $\phi_i(t)$ is a gaussian variable with zero mean and variance

$$\langle\phi_i(t)\phi_i(t)\rangle = \frac{2T}{\Gamma_0}\delta(t-t') + J^2C(t-t') \; . \tag{9}$$

The detailed treatment done in [13] cannot be repeated in the case $k \neq 0$, where things become too complicated. On the contrary the spherical model, or p-spin model (here with $p = 2$), can still be treated in a satisfactory way. The spherical model (than can be seen as a mean field of the mean field, or, simply, as a different model from SK) can be defined trough the Langevin equation

$$\Gamma_0^{-1}\frac{\partial}{\partial t}\sigma_i(t) = -r\sigma_i(t) + \sum_j J_{i,j}\sigma_j(t) + h_i(t) + \xi_i(t) \; , \tag{10}$$

where we have only kept the quadratic part of the potential (that had been already extracted in the r-term in (3), and where now the parameter r is not a free parameter but such that

$$\frac{1}{N}\sum_i \sigma_i(t)^2 = 1 \; . \tag{11}$$

In this approach one easily checks that for the symmetric model, $k = 0$, $\chi = \frac{1}{T}$ for $T > T_g$ (where T_g is the first temperature where q takes a non-zero expectation value). There is a spin glass transition at $T_g = 1$, and $\chi = 1$ for $T \leq T_g$.

For the asymmetric case $k \neq 0$ at finite T one finds that there cannot be any transition (we will not discuss here about what happens at $T = 0$, since in our numerical simulations we always investigate the system at finite T): $q = 0$ for all $T > 0$. The reason is that $G(\omega)$ is singular when $\chi^2 = \frac{1-k^2}{1+k^2}$, while $C(\omega)$ is singular at $\chi = 1$. That implies that χ stops at 1 in order not to violate finiteness of correlation functions.

At last we recall that [1] finds that for small k the correlation time τ diverges like

$$\tau \simeq k^{-6} \; . \tag{12}$$

The way of reasoning that we have explained two paragraphs ago would also suggest (as found by Hertz, Grinstein and Solla in [3]) that the same thing happens in the full SK mean field model. But in the case of the SK model this is only a qualitative argument: for example replica symmetry breaking could change things: for example Crisanti and Sompolinsky [1] discuss the possible appearance of a hierarchical distribution of large correlation times, and of a slow component not only in $C(\omega)$ but also in $G(\omega)$. In the rest of this note we will study the case of the full fledged SK model, in the regime where the Parisi solution characterizes the symmetric model.

Cugliandolo, Kurchan, Le Doussal and Peliti in [12] have found that the result of [1] is valid also when one does not assume a priori time translational invariance [14], for a p-spin model with $p > 2$. They are interested in the behavior of the p-spin model for $p > 2$ (that is non-marginal, and in some sense more general than the SK model). They also find that (for $N < \infty$) in the p-spin model there are deep stable states that show a complex dynamical behavior even in the non-symmetric case.

At last we note that Parisi [4] has proposed to use spin glass systems with non hamiltonian perturbation as a way to build memories that can be confused, and has suggested that the asymmetry can be crucial for the process of learning.

3 Definitions

We will give here all the definitions that are relevant for the model discussed in this paper. We consider an infinite range model, based on spin variables $\sigma_i = \pm 1$, where $i = 1, \ldots, N$ labels site. The couplings $J_{i,j} = \pm\frac{1}{\sqrt{N}}$ with uniform probability (both the symmetric couplings $J_{i,j}^{(S)}$ and the non-symmetric ones $J_{i,j}^{(NS)}$). The usual Sherrington Kirkpatrick version of the mean field spin glass is defined by a probability distribution for the spin variables built over a Hamiltonian

$$P(\{\sigma\}) \simeq e^{-\beta H} = e^{\beta \sum_i \sigma_i \sum_j J_{i,j}^{(S)} \sigma_j} \equiv e^{\sum_i \sigma_i F_i} \ , \tag{13}$$

where the $J_{i,j}^{(S)}$ are the usual quenched, symmetric random variables, with $J_{i,j}^{(S)} = J_{j,i}^{(S)}$.

We run a local dynamic, usually known as *Heat Bath*: each spin σ_i is in turn equilibrated with the field given by the other spins. The probability for the new spin σ_i to be $+1$ after the update is

$$P(\sigma_i = +1) = \frac{e^{F_i}}{e^{F_i} + e^{-F_i}} \ . \tag{14}$$

We measure the expectation value (thermal and over the disorder) of the internal energy at time t

$$E(t) = \frac{1}{N} \overline{\langle \sum_i \sigma_i F_i \rangle} \ . \tag{15}$$

We always follow two copies (α and β) of the system in a given quenched realization of the couplings, and we compute the overlap

$$q(t) \equiv \frac{1}{N} \langle \sum_i \sigma_i^{(\alpha)} \sigma_i^{(\beta)} \rangle \ . \tag{16}$$

In the non hamiltonian case one updates the spins under the field

$$F_i \equiv \beta \frac{1}{\sqrt{1-2\epsilon+2\epsilon^2}} \sum_j [(1-\epsilon) J_{ij}^{(S)} + \epsilon J_{ij}^{(NS)}] \sigma_j \equiv F_i^{(S)} + F_i^{(NS)} \ , \tag{17}$$

where now $J_{i,j}^{(NS)}$ is drawn independently from $J_{j,i}^{(NS)}$, and we have called $F_i^{(S)}$ the part of F_i proportional to $J^{(S)}$ and $F_i^{(NS)}$ the part proportional to $J^{(NS)}$. This is the model we will analyze in the following. ϵ and k of [1] have the same scaling behavior when they are small, and play the same role.

In the case of the non hamiltonian extension of the dynamics we also measure separately the symmetric and the non-symmetric contributions to the energy, i.e.

$$E^{(S)}(t) = \frac{1}{N} \overline{\langle \sum_i \sigma_i F_i^{(S)} \rangle} \ ; \quad E^{(NS)}(t) = \frac{1}{N} \overline{\langle \sum_i \sigma_i F_i^{(NS)} \rangle} \ . \tag{18}$$

We define the time dependent correlation function

$$c(t_w, t_w+t) \equiv \frac{1}{N} \sum_{i=1}^{N} \overline{\langle \sigma_i(t_w) \sigma_i(t_w+t) \rangle} \ . \tag{19}$$

We measure the correlation functions $c(t_w, t_w+t)$ for all t_w and t of the form 2^n, with n integer. All the data analysis we will describe in the following will be based on the knowledge of the $c(t_w, t_w+t)$ at these times.

To try to quantify how large is the effect of a given ϵ value we plot in fig. (1) the expectation value of the total energy operator (empty dots), of its symmetric part (filled dots) and of the non-symmetric part (plus symbols). Error bars are smaller than the symbols. There is an important difference distinguishing data at $T = 0.2$ from the ones at $T = 0.5$ (all taken from averages over the last two thirds of our total Monte Carlo sweeps). Data at $T = 0.5$ on a small lattice, $N = 256$, are at equilibrium, in the sense that their average does not depend anymore on time. On the contrary data at $T = 0.2$ are for some ϵ values out of the equilibrium (see fits later on): but this is a small effect, not relevant for the point we are doing here. At $\epsilon = 0.0$ obviously the total energy coincides with the symmetric contribution, while the non-symmetric part is zero by construction. As ϵ becomes different from zero the non-symmetric part acquires a non-zero expectation over the dynamics: at $\epsilon = 0.1$ it stays very small, while at $\epsilon = 0.5$ it is of the same order of magnitude than the symmetric contribution. The $T = 0.2$ and $T = 0.5$ cases look from fig. (1) very similar.

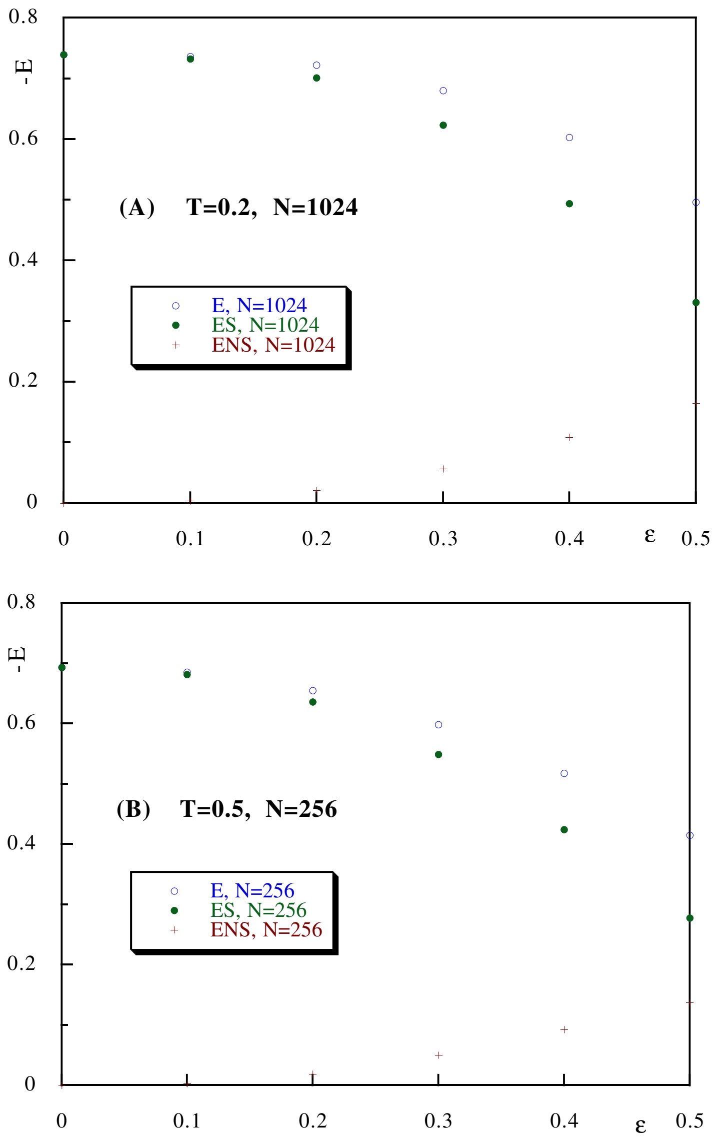

Figure 1: Expectation values of the total energy operator, of the symmetric part and of the non-symmetric part as a function of the asymmetry parameter ϵ.

The computer runs discussed in this paper have taken a few months of computers of the class of a Pentium 133 or of a 3000/300 Digital α Unix workstation.

4 Aging

At first we will try to understand the dynamical behavior of such systems, by studying aging phenomena [15]. We will start by looking, as a reference point, to the usual hamiltonian SK model.

We will look as usual at the time dependent correlation function $c(t_w, t_w + t)$. Our *dynamical* runs (where we do not try to reach thermal equilibrium) have been done at $T = 0.2$ (for the SK model, $\epsilon = 0$, $T_c = 1$). We have studied systems with different number of sites, up to $N = 1024$ (the case we will discuss in the following). For $N = 1024$ we have 20 samples for each different ϵ values.

In fig. 2 we plot $c(t_w, t_w + t)$ as a function of t, for different values of t_w (lower curves depict smaller t_w values). Here $N = 1024$, $\epsilon = 0$ (i.e. the hamiltonian case of the usual SK model). Error bars come from sample to sample fluctuations. The system starts from a disordered configuration, and we let it evolve. The fact that the correlation function is not time-translational invariant is very clear: $c(t_w, t_w + t)$ is not a function of t only. For small values of t_w the system decays fast, and the decay rate slows down when one looks at high values of t_w.

We are here in the same situation of [16] for the simulations of the hypercubic model: on the observed time scales $q^2(t)$ (as measured from two copies of the system in the same noise realization) stays small ($\leq .04$). The system has not crossed the very high barriers that is encountering on his way. We will discuss that better in the followings sections, together with the fact that the energy is decaying to its asymptotic value with a very good power law (at $\epsilon = 0$ and $N = 1024$ the exponent is of order 0.4).

In fig. 3 we plot the same data as a function of $\frac{t}{t_w}$ (again in double log scale). This is the usual search for an aging-like scaling. Here the scaling of the data is reasonable but obviously not perfect: scaling violations are clearly present, but a detailed study of this phenomenon is beyond the scope of this study. The plateau (to be) for $t < t_w$ is connected to the value of the same state overlap q_{EA}[1] (see [17] and figures 3 to 5 of [18]). We remark that these results are compatible with the ones obtained by Rossetti [19] on very large lattices (SK model up to $N = 8192$) and (when looking in details at the graphs: the aging curves tend to separate soon after the crossing point for all values of t_w) with the ones obtained by Cugliandolo, Kurchan and Ritort on the alternative, hypercubic definition of the mean field [16]. We just repeat that violations of a perfect aging scaling are here quite clear. Definitely the usual Sherrington Kirkpatrick model does not show any easily explainable form of scaling.

[1] We thank Juan Ruiz-Lorenzo for an interesting conversation about this subject.

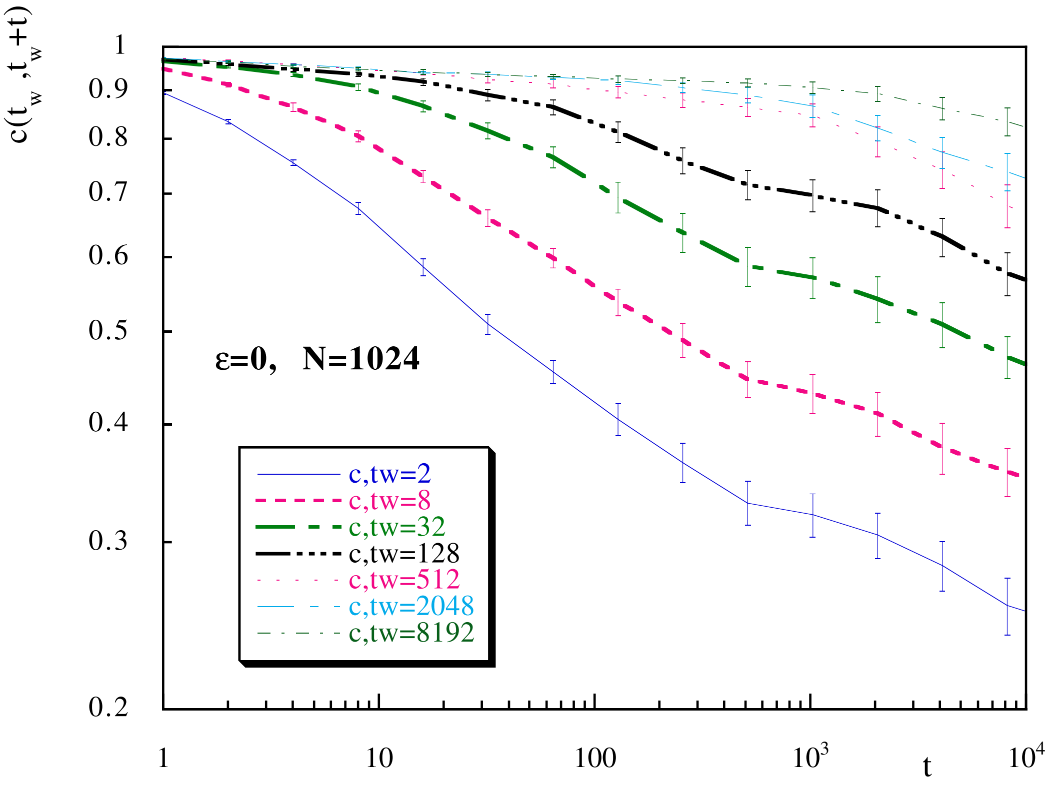

Figure 2: The spin-spin time dependent correlation functions $c(t_w, t_w + t)$ as a function of t, for different values of t_w (lower curves for smaller t_w values). 20 samples, $N = 1024$, $\epsilon = 0$ (i.e. the hamiltonian case of the usual SK model). Error bars are from sample to sample fluctuations. Log-log scale.

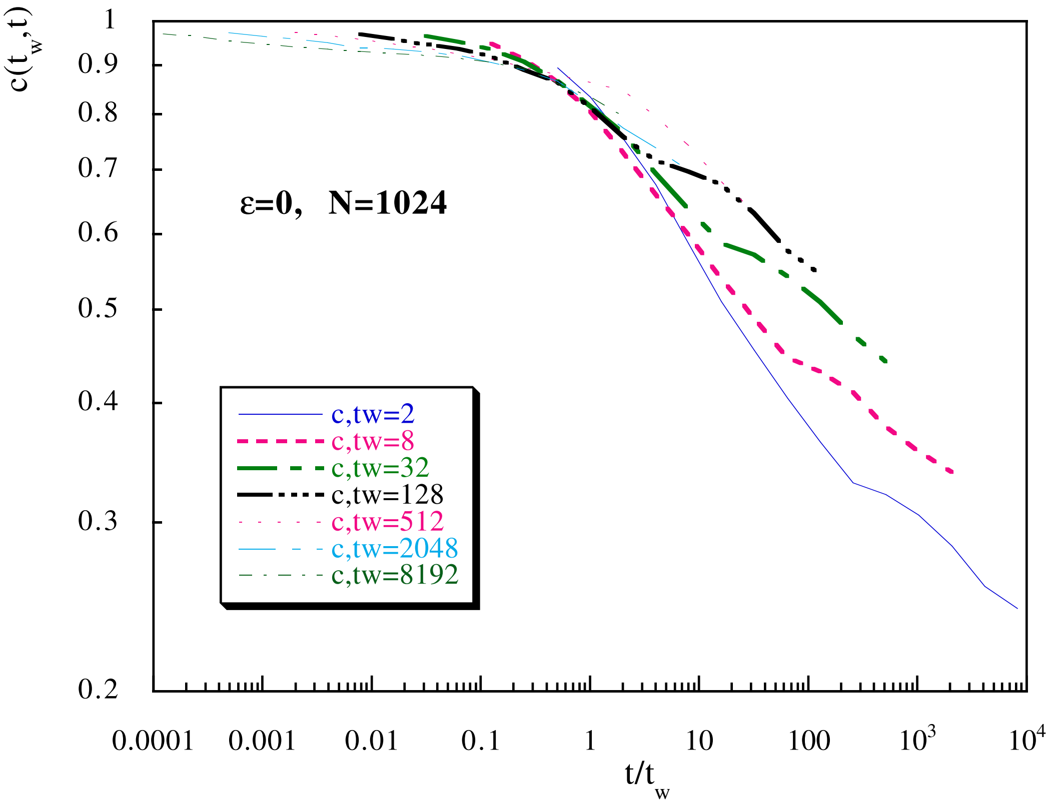

Figure 3: As in fig. 2, but versus $\frac{t}{t_w}$.

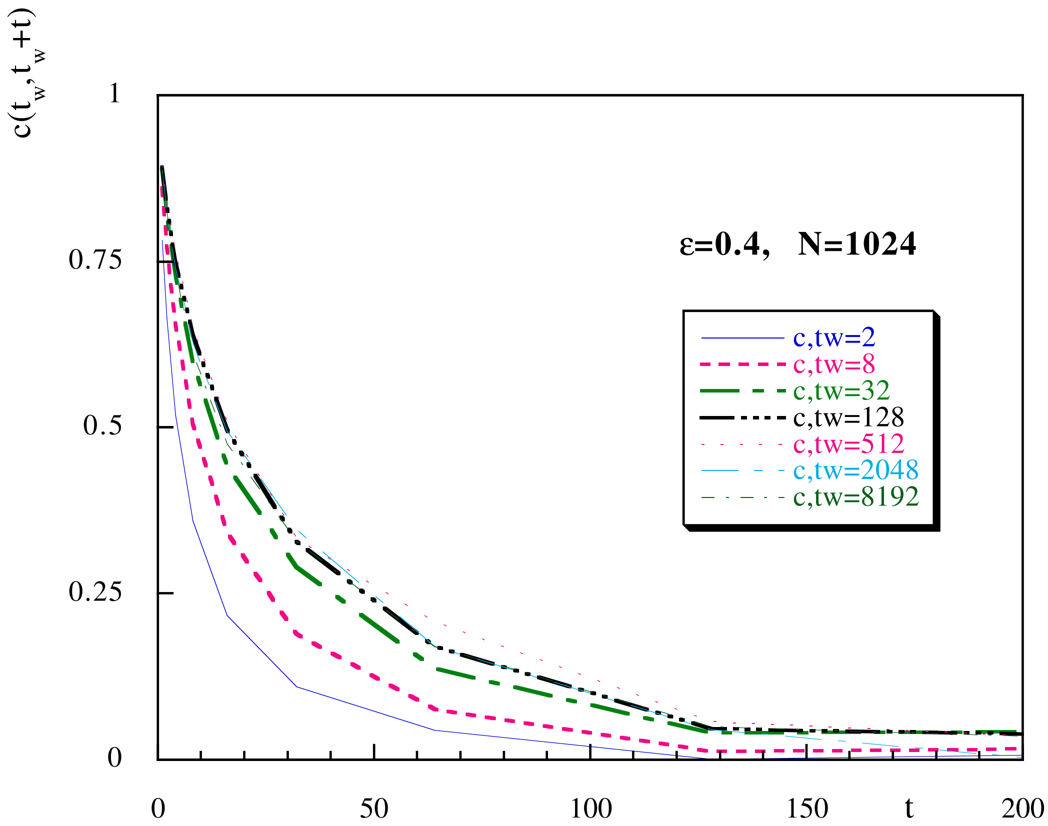

Figure 4: As in fig. 2, but $\epsilon = 0.4$, and linear-linear scale.

We will try now to analyze what happens in the non hamiltonian dynamics. We start with the non hamiltonian dynamics by looking at a large perturbation: we use $\epsilon = 0.4$, 20 samples and $N = 1024$. In fig. 4 the correlation functions for different values of t_w (here in simple linear-linear scale). It is clear that things are now very different. The decay at very small waiting times is faster than for larger t_w, but already for $t_w \leq 32$ there is very little dependence of c over t_w. The curves from different t_w are collapsing on a same universal decay curve.

Since we are maybe expecting here an exponential decay of the time dependent correlations (but we will see this is a far from evident fact) we plot in fig. 5 the correlation functions for different values of t_w in linear-log scale. Here we also include the error from sample to sample fluctuations. The lines would be asymptotically straight lines in case of an asymptotic exponential decay. The careful reader can start to observe that in this case ($\epsilon = 0.4$) in all the time range where we can determine an *effective* t dependent correlation time $\tau_e(t)$ (by looking for example at the local slope of the logarithm of the correlation function), such $\tau_e(t)$ is increasing (i.e. the curves are bending up in all the region where we have been able to determine them with good statistical precision).

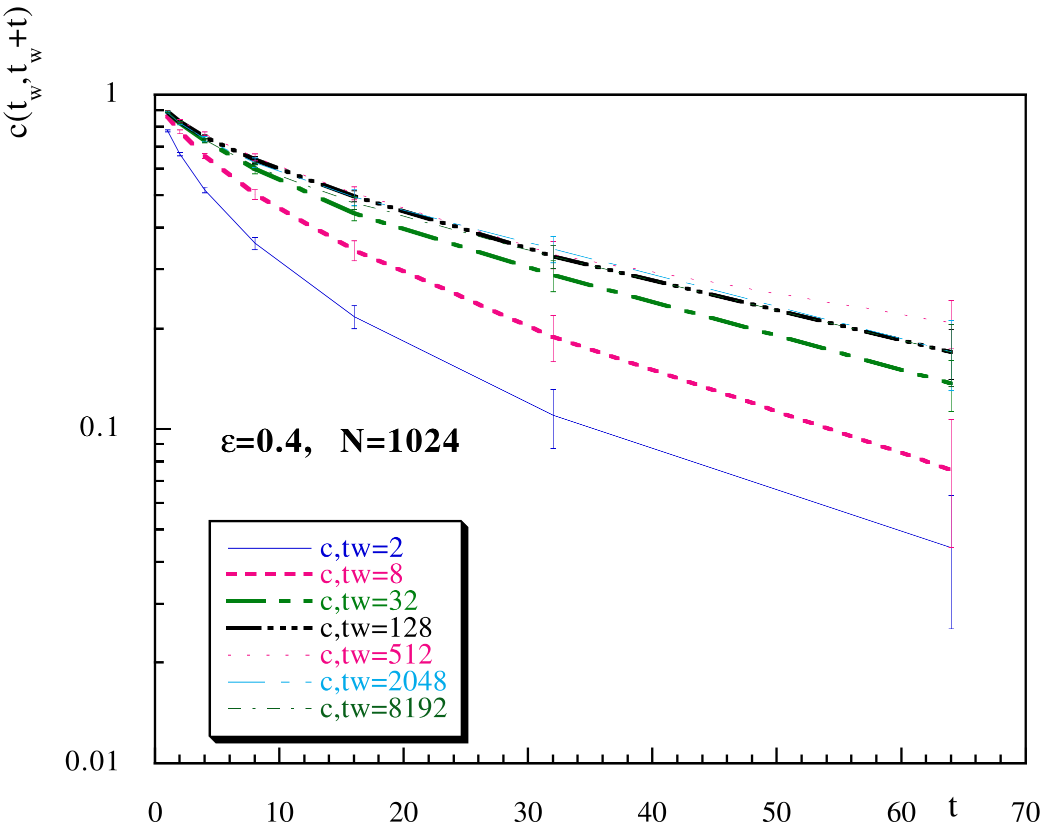

Figure 5: As in fig. 2, but $\epsilon = 0.4$, and linear-log scale.

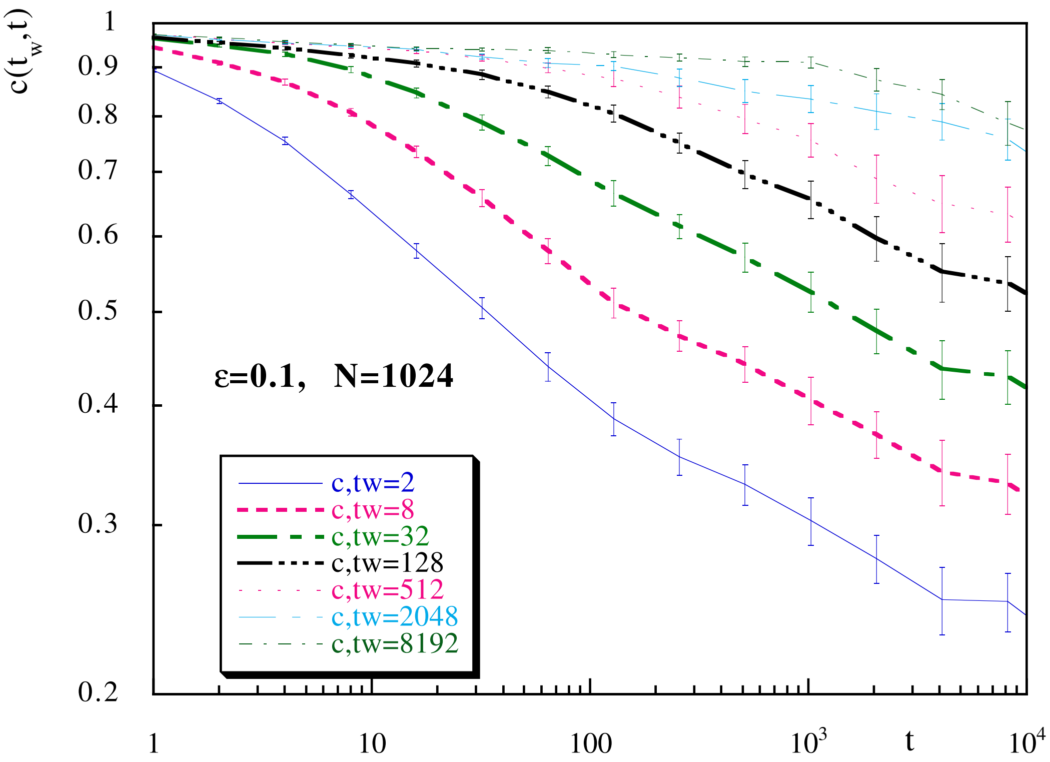

Figure 6: As in fig. 2, but $\epsilon = 0.1$.

Other data for ϵ going from .3 to .5 give very similar hints. A first conclusion can be reached at this point: systems with large non hamiltonian perturbations do indeed have a quite different, typically non-aging, dynamical behavior, but one has to be careful since it looks difficult to pin point a real exponential decay.

Let us now turn to a reasonably small value of the non hamiltonian perturbation. We select $\epsilon = 0.1$, that is not too small: the non-symmetric couplings are coupled with a strength .1 times β while the symmetric couplings interact with a strength of .9. These data turn out indeed to be dramatically similar to the ones at $\epsilon = 0$. In figures 6 and 7 the analogous of figures 2 and 3: the similarity is self-explanatory. Later on we will try to quantify the differences and to elucidate their meaning. By now we observe that for large lattices ($N = 1024$ for the infinite range model is a large lattice, since one has one million of couplings) and long times (we follow the system up to t and t_w of order 16384) the model with $\epsilon = 0.1$ shows an aging behavior as good as the one ever observed for the pure SK model.

Before discussing a more quantitative analysis of these data, a few comments about an intermediate case, $\epsilon = 0.2$. Here the pattern of $c(t_w, t_w + t)$ is different from both the usual aging case (like the one we find for $\epsilon = 0.0, 0.1$) and the typical fast decay to an equilibrated state (see $\epsilon = 0.4$, even if we will see that

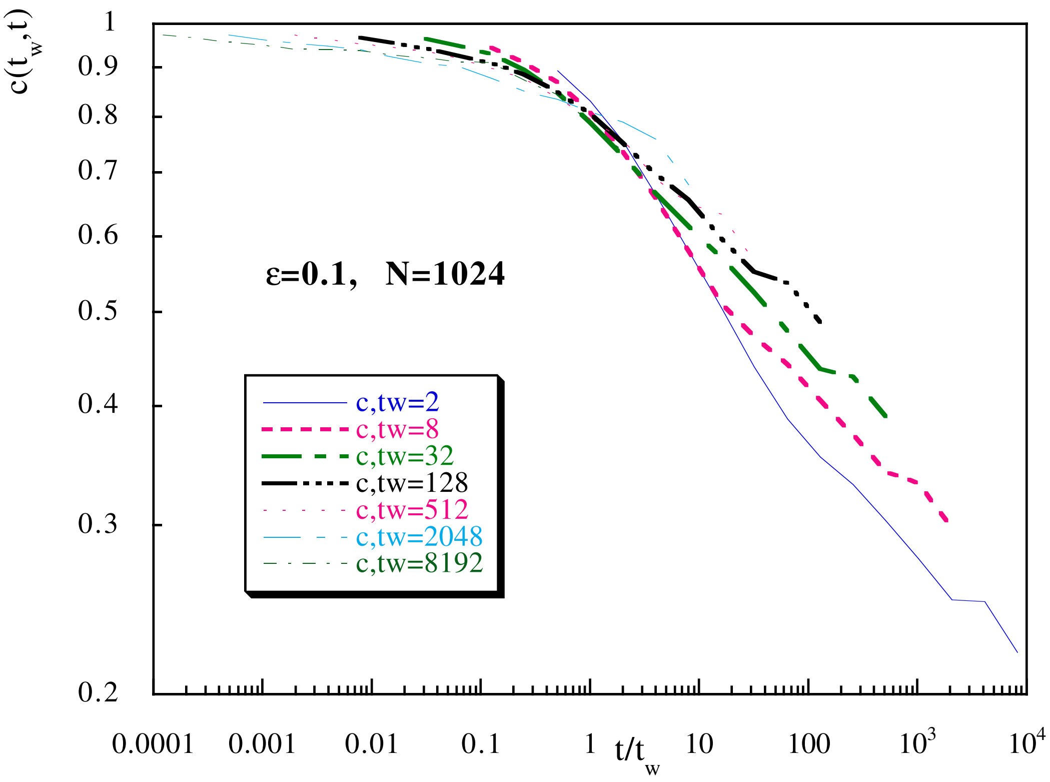

Figure 7: As in fig. 3, but $\epsilon = 0.1$.

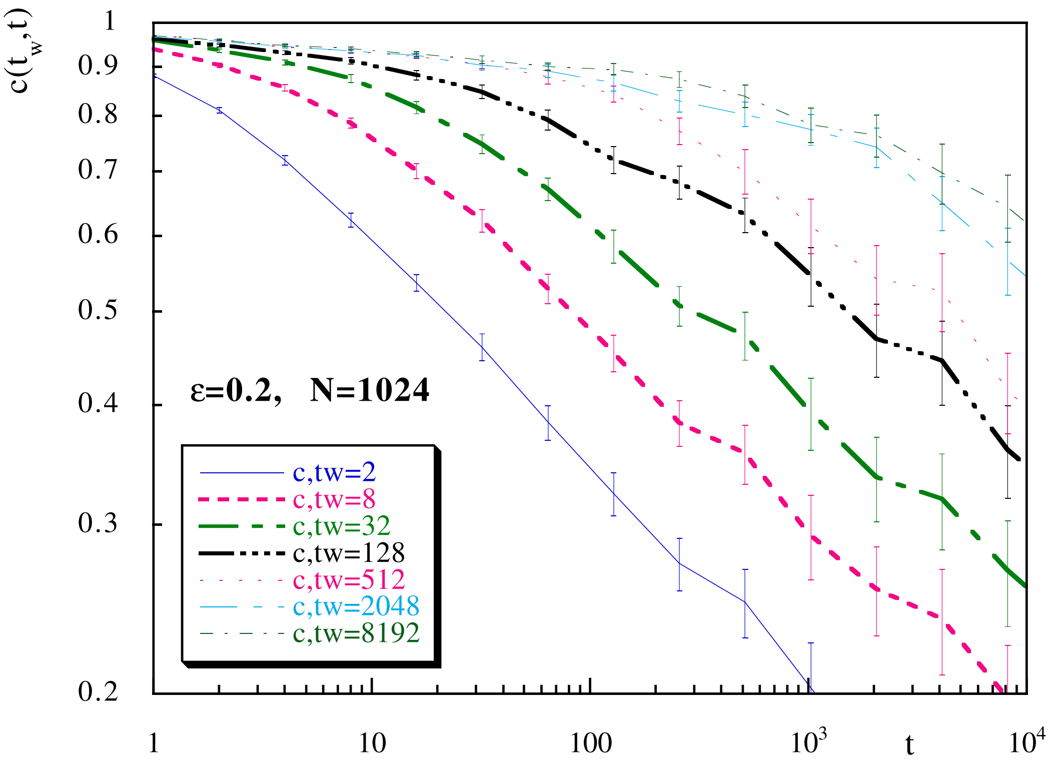

Figure 8: As in fig. 2, but $\epsilon = 0.2$.

even here things are more complex).

In figure 8 the correlation function as a function of t. The pattern is reminiscent of an aging pattern, even if for large t_w the situation is not so clear. The plot of c versus $\frac{t}{t_w}$ in fig. 9 is more innovative: here the typical crossing one expects at $\frac{t}{t_w} \simeq 1$is moved to larger values of $\frac{t}{t_w}$, which increase with t_w. The scaling is different from the one of the hamiltonian case.

It is interesting to note, as a basis of a discussion we will present in one of the next paragraphs, that this is not only an effect we detect at high t_w values. Already for very short t_w (2 and 8, for example) we find a crossing at t of order 10. We also want to notice that, looking at their value, in the region $t > t_w$ the $\epsilon = 0.2$ data seem to show a better pure $\frac{t}{t_w}$ scaling than the pure ones: but this is probably a non very relevant feature (that could be typical of a transient behavior).

The similarity of the correlation functions in the pure SK model and the ones in the model with $\epsilon = 0.1$ calls for a better scrutiny. The very remarkable similarity of the two sets of functions has to be quantified in some way. In order to do that we compute the ratios of the correlation functions at the same t and t_w with $\epsilon = 0$ and $\epsilon = 0.1$, and we plot them in fig. 10. The correlation functions are indeed very similar, but for increasing values of $\frac{t}{t_w}$ we start to see a small

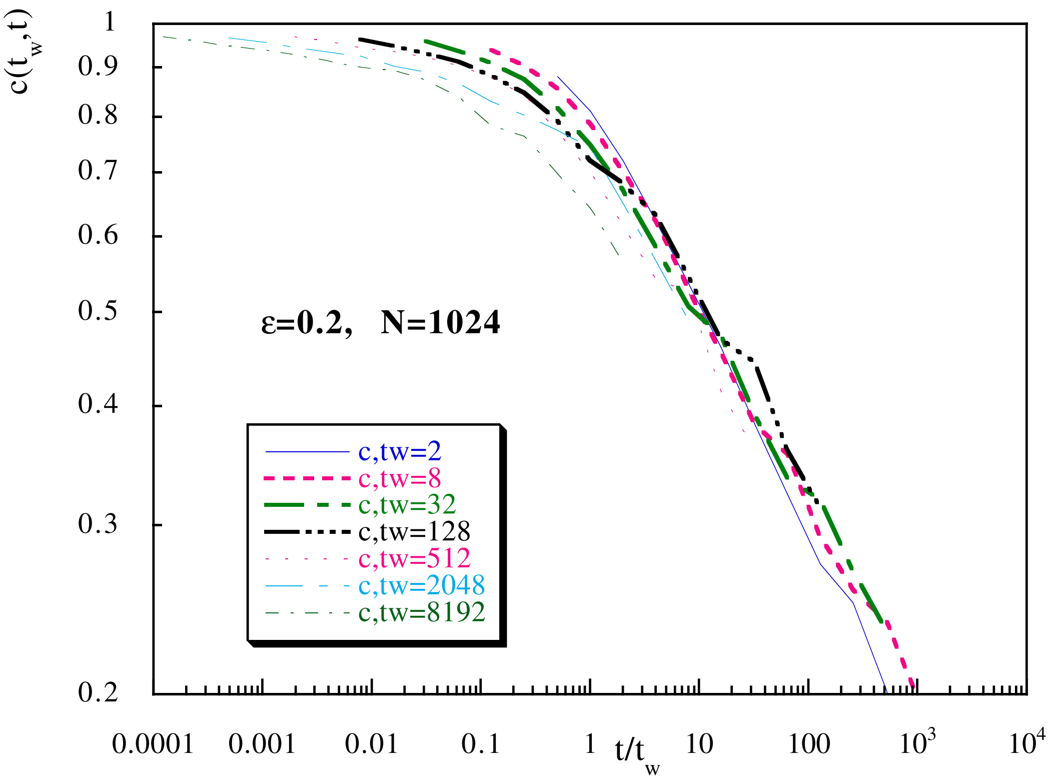

Figure 9: As in fig. 3, but $\epsilon = 0.2$.

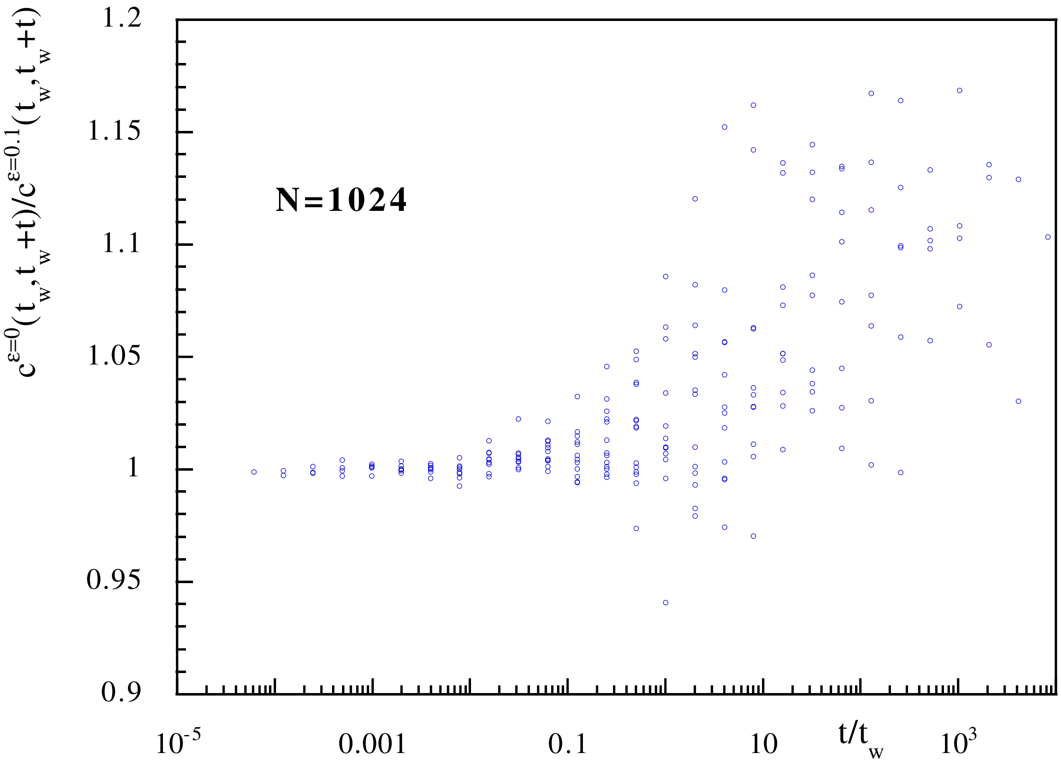

Figure 10: The ratios of $c(t_w, t_w + t)$ at the same t and t_w with $\epsilon = 0$ and $\epsilon = 0.1$ versus $\frac{t}{t_w}$ in linear-log scale.

difference (typically the higher points at fixed $\frac{t}{t_w}$ are for higher t values). We do not plot the statistical errors, which would blur the plot in an extreme manner, but even if any individual ratio is compatible with one, the large time growth of the ratios is clear and statistically significant: at large times the correlations for $\epsilon = 0.1$ case start to decrease faster than for the pure SK case. It is a very small effect, and its meaning is not unambiguous: it could signify that we are exiting a transient phase and aging is ending, or it could just be an irrelevant renormalization (a shift of the effective temperature of the system). But the effect is clear, and we note it here.

In fig. 10 we plot the same ratio, but here $\epsilon = 0$ is divided times $\epsilon = 0.2$. Note that the vertical scales of this and the former plots are very different. Here the faster decay of the non hamiltonian case is very clear: for $\frac{t}{t_w}$ of order 10^4 the ratio is of order two.

Two remarks: first the departure from a ratio close to unit comes for the $\epsilon = 0.1$ case quite late.The departure from unit is far more pristine at $\epsilon = .2$. For example one can notice that a value of 1.05 is reached at $t/t_w \simeq 10$ in the first case, and of order $10^{-3} - 10^{-2}$ in the second case.

If one tries in this way a very qualitative definition of an ϵ dependent correla-

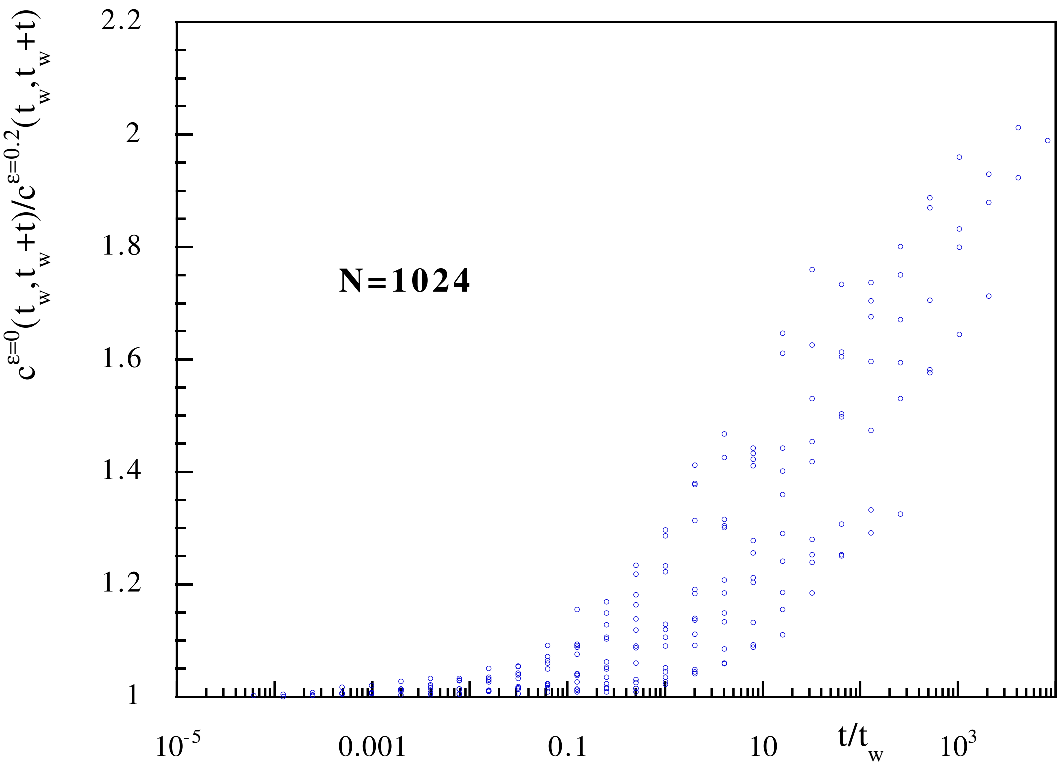

Figure 11: As in fig. 10, but $\epsilon = 0$ over $\epsilon = 0.2$.

tion time one gets a divergence that is faster than the one one would get with an ϵ^{-6} scaling (see later). It should also be noticed that this effect is not dominated by finite size effects: on different volumes we get very similar results.

The next natural thing to do is to check for correlation times. The Crisanti-Sompolinsky [1, 2] result for the spherical model hints for a behavior

$$\tau \simeq \epsilon^{-6} , \tag{20}$$

and one can proceed by trying to support or falsify this expectation. In this case one would start from the larger ϵ values, where the asymptotic decay looks better exposed, and try to go down to lower ϵ values.

Determining correlation times is typically not as easy as one expects. The main caveat is indeed that in a numerical simulation at her best one can establish upper bounds on correlation times: correlation times that are larger than the simulation time cannot be detected. In the case of systems which exhibit (or could exhibit) an aging behavior things are even more complex since a priori one cannot average over t_w. Only after checking that we are in a region of time translational invariance we are allowed to average over different waiting times.

The first, easy approach, consists in defining the correlation time as the time after which the time dependent correlation function reaches, down from 1, a given value, say $\tilde{c}$. In fig. 12 we plot the time needed for c to reach the value .7, and ϵ^{-6} as a function of ϵ (we have also done the same analysis for $\tilde{c} = .5$). It would be incorrect to average over t_w's: only a posteriori, after checking that we are in an asymptotic region of a simple phase where time translational invariance holds, that would be justified. We have checked indeed that doing that can lead to a false scaling. In fig. 12 we have only used the largest t_w points available to us ($t_w = 2^{14}$). We have normalized the data in the plot such that the data points coincide at the higher ϵ value ($\epsilon = 0.5$). It is clear that already at $\epsilon = 0.3$ the ϵ^{-6} scaling does not hold (we are using a double log scale!). At $\epsilon = 0.2$ the discrepancy from an ϵ^{-6} scaling is severe, and for $\epsilon = 0.1$ we cannot determine τ since the correlation function with $t_w = 2^{14}$ does not reach the value of 0.7. Anyhow here τ would be so huge to be completely incompatible with an ϵ^{-6} scaling.

When using a lower threshold (that should underestimate less the true correlation time) the situation is even more dramatic. In this case we can only determine τ for $\epsilon \geq 0.3$, and the deviation from an ϵ^{-6} scaling is more severe.

From this first, very naive analysis, we can already conclude that if we could define a correlation time τ for $\epsilon \to 0$ it would be growing far more dramatically than like ϵ^{-6}. The analysis of section (VI.A) [2] is in this sense probably incorrect since the authors average the correlation function over small t_w values (but they are working in conditions not identical to us, both because the exact form of the non hamiltonian contribution to the force and since they are at $T = 0.5$).

Since the question of correlation times, of their scaling behavior and of the

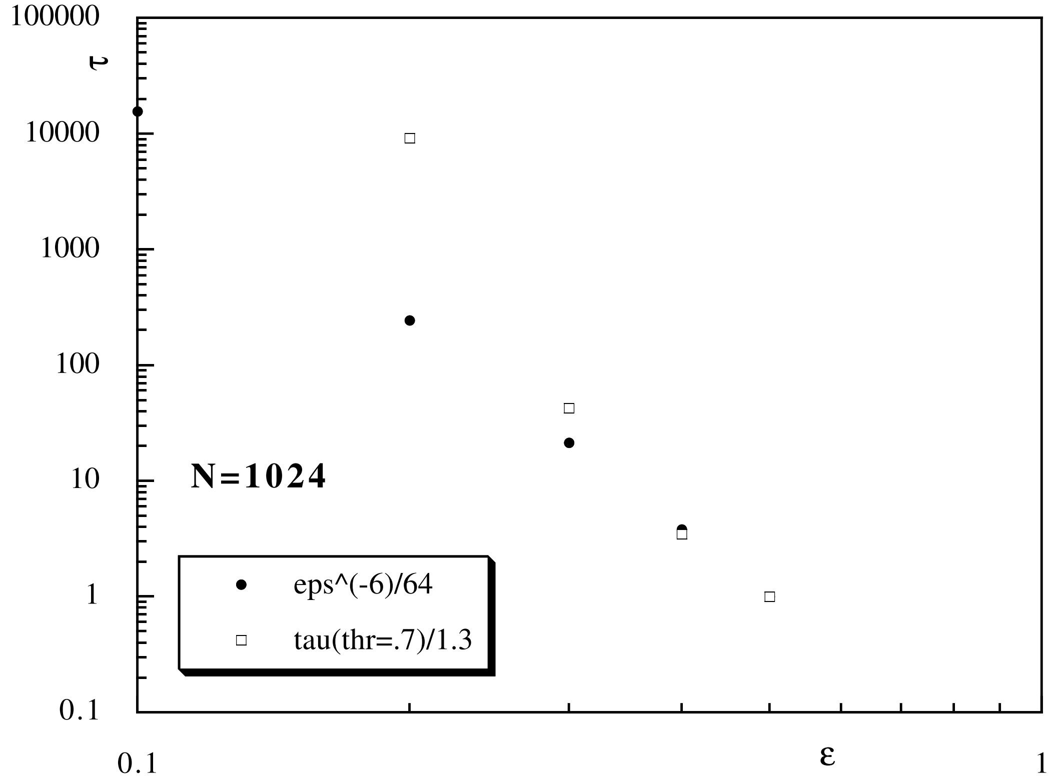

Figure 12: As a function of ϵ, in double log scale, we plot the time needed from c to reach the value .7, and ϵ^{-6}.

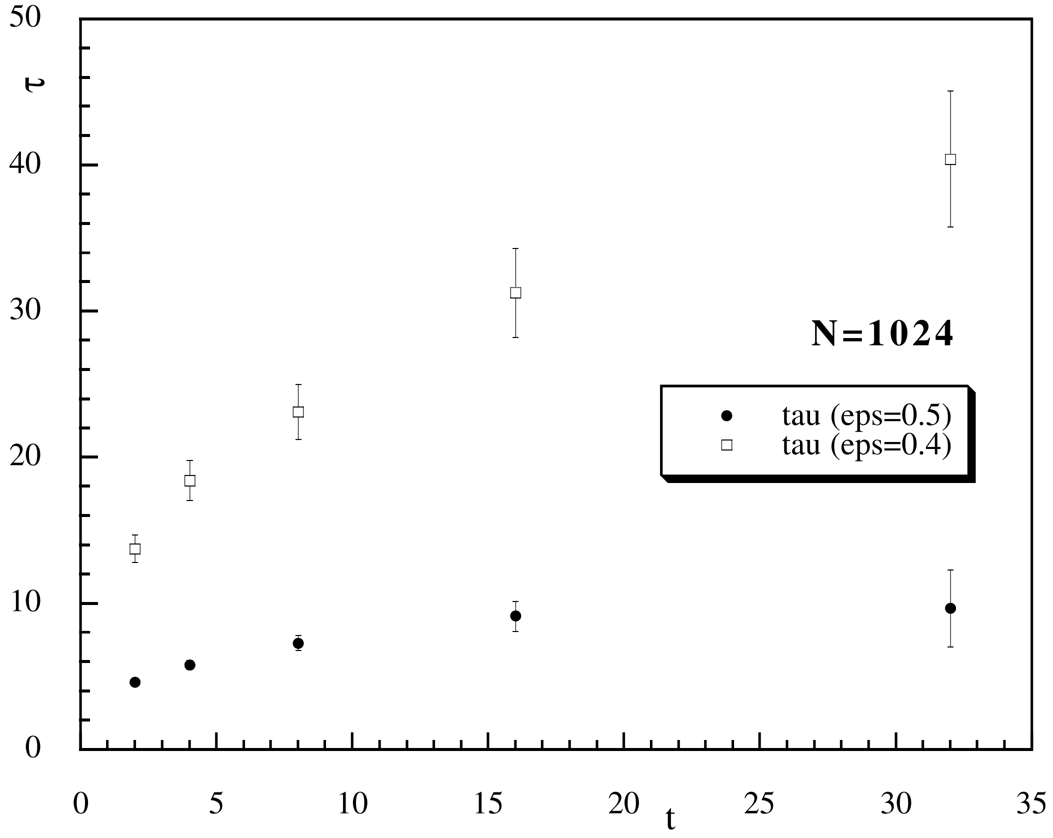

Figure 13: $\tau_{eff}(t)$ versus t for $\epsilon = 0.5$ and 0.4.

functional form of the time dependent correlation functions of the non hamiltonian system is of crucial interest, we have decided to perform a careful analysis of this issue. The standard approach for trying to expose clearly an asymptotic exponential behavior is based on the definition of a time dependent effective correlation time $\tau_{eff}(t)$. If we are in the asymptotic large time regime of a phase with an exponential decay of time-dependent correlation functions

$$c(t) \simeq A e^{-\frac{t}{\tau}} \ , \tag{21}$$

and

$$\tau_{eff}(t) \equiv \Big(\frac{1}{t}\log(\frac{c(t)}{c(2t)})\Big)^{-1} = \tau \ . \tag{22}$$

$\tau_{eff}(t) \to \tau$ at large times.

We have hinted before that already figure 5 suggests that we cannot, from the data from our numerical simulations, exhibit a clean exponential behavior even at $\epsilon = .4$. In fig. 13 we plot $\tau_{eff}(t)$ versus t for $\epsilon = 0.5$ and 0.4.

We have averaged curves for different t_w in the region where the dependence over t_w is smaller than the statistical error (16 for $\epsilon = 0.5$, 64 for $\epsilon = 0.4$, 512 for $\epsilon = 0.3$, 2048 for $\epsilon = 0.2$, while for $\epsilon = 0.1$, 0.0 we have only selected the largest t_w). We plot the larger ϵ values since for lower ϵ it is quite clear we are not observing at all an exponential decay. But, as we said, already for large ϵ the effective correlation time steadily increases, as a function of t, in the time region we can handle safely. It is not clear from our data if $\tau_{eff}(t)$ is maybe reaching a plateau, but it is clear that where we can determine it with good precision it has not reached an asymptotic value.

We have also tried global fits to an exponential decay, by changing the number of data points used in the fit. They are quite bad for all ϵ values (but maybe at $\epsilon = 0.5$ where the noise threshold is reached after only a few data points). If discarding enough points close to the origin maybe an exponential fit is preferred at $\epsilon = 0.5$ and 0.4, while a power fit is preferred at $\epsilon = 0.3$. For lower ϵ values one cannot find a simple behavior that fits well the data.

The evidence presented in this section does not completely clarify the main issue. On the time scales we can observe there is still aging for small non hamiltonian perturbations, while for large perturbations aging disappears. Still, even in the case of large perturbations a pure exponential behavior is slow to emerge. Somehow it is clear that we are dealing with a system with a very complex dynamics, even if it is difficult to establish if we are dealing with a transient behavior or with an asymptotic effect. But complexity is strong, and manifests itself with different signatures we have discussed in some details, in all the parameter range we have explored. If we try to define a correlation time, even where it is not clear we could define one, it turns out to diverge faster than what a spherical spin model analogy would predict. That could be connected to a signature of the replica symmetry breaking pattern of the Parisi solution.

Maybe the most important question we are not able to answer in a precise way is: is something drastic happening when going from large non hamiltonian perturbations (where we know that we will eventually get a non-aging behavior) to small perturbations? It is very difficult to discriminate among a transient behavior on a very long time scale and a true asymptotic behavior. If any, our feeling about this issue is that yes, things at $\epsilon = 0.1$ are different from things at $\epsilon \geq 0.2$. This is based both on the scaling of $\tau(\epsilon)$ we have discussed before (that is not compatible even with the very high power predicted by the spherical spin model solution), and by a hand-waving argument we give now. Let us be very conservative and say that $\tau(\epsilon = 0.2)$ is of order 300 (this is by far a lower bound, and τ is probably, if any, far larger than that), and $\tau(\epsilon = 0.1) > 10000$ (this is obvious). At $\epsilon = 0.1$ for all times in our measurement windows ($O(2^{14})$) we see a very good aging. Than we would expect that at $\epsilon = 0.2$ at least for $t \ll 300$ we should have a transient aging, that could die out later on. We do not have that at all. Already at $t_w = 2, 4$ aging curves at $\epsilon = 0.2$ behave in a way that is dramatically different than for usual aging. The argument of the transient behavior was used in [1] to describe the situation at finite ϵ, and it surely works for the spherical spin model: but here we have evidence that the argument does not apply.

Because of that, of the wrong scaling and of the further evidence we will present in the next section we cannot exclude that something changes at a critical value of ϵ.

5 Power Laws

Slow relaxation toward thermal equilibrium expectation values is one of the typical signatures of disordered systems. First Gardner, Derrida and Mottishaw [20] have pointed out and quantified this kind of effect in spin glasses. Eisfeller and Opper [21] have introduced a powerful dynamical functional method that allows to compute with good precision the power exponents at $T=0$. Ferraro [22] has generalized this work to $T \neq 0$. Work based on numerical simulations [19, 23, 24] has made these computations detailed: one can determine with a reasonable accuracy power exponents even at $T \neq 0$, both for the remnant magnetization and for the energy decay.

We have used the decay toward equilibrium of typical observable quantities (like the internal energy $E(t)$ and the squared overlap $q^2(t)$) as a probe of the existence of a complex behavior even for the non hamiltonian, $\epsilon \neq 0$ case. We have measured and tried to fit the time dependent internal energy

$$E(t) \simeq E_\infty + A t^{-\eta} \ , \tag{23}$$

and analyzed the slow growth of $q^2(t)$ towards its equilibrium value. On general ground we notice that the exponents we have determined for the energy are quite stable: they do not seem to depend much over the lattice size (we have checked different sizes) and over the time window we use to fit them.

First we present the results from our runs at $T=0.2$, the same we have discussed in the former section of this note. We start from $E(t)$. At $\epsilon=0.0$ and $\epsilon=0.1$ a power fit is perfect, while an exponential decay is clearly ruled out. In fig. 14 we plot the data with the best fits for $\epsilon=0.0$ and $\epsilon=0.1$. The error is here of 1 to 3 on the last digit. It is clear that the two sets of data are compatible in the statistical error: a small shift in the effective temperature of the system is the best way to explain the small shift in the data (the situation will be similar for higher T values). Also at $\epsilon=0.2$ and 0.3 we get a perfect power fit, with an exponent of .39 and .48 respectively, and an exponential behavior is ruled out. $\epsilon=0.4$ is an intermediate case, where both a power fit (that would give an exponent of .63) and an exponential fit are not very good. At $\epsilon=0.5$ the exponential fit is definitely better, and the energy clearly reaches its asymptotic value.

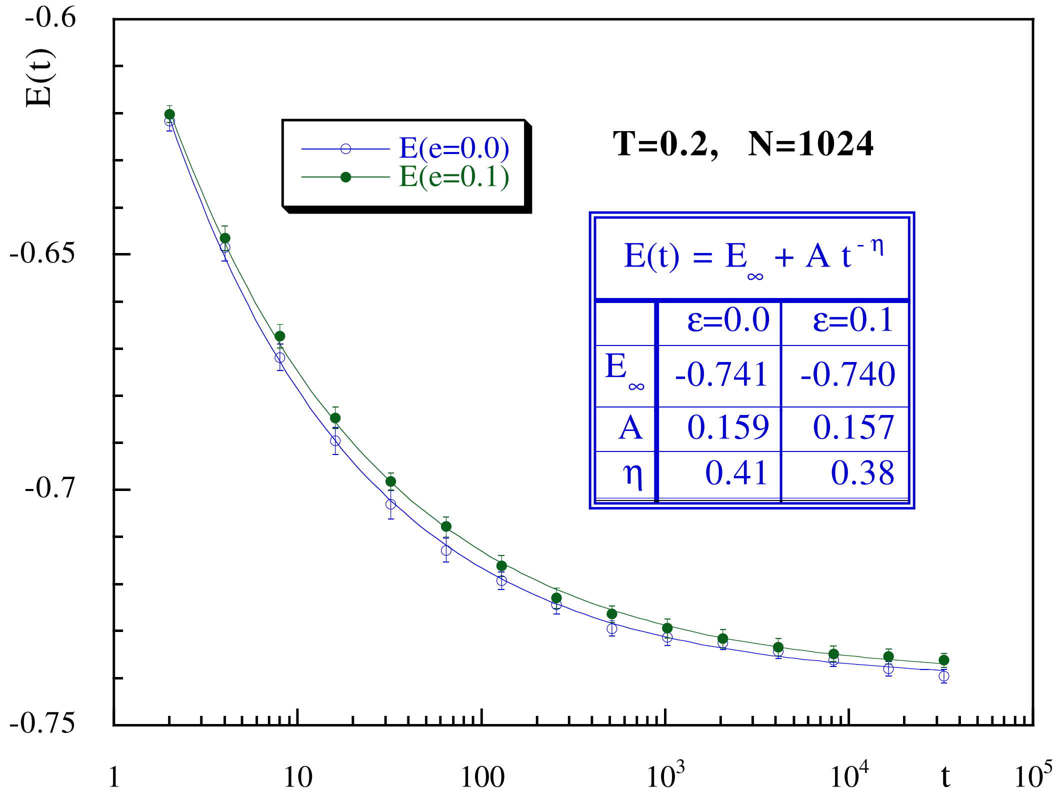

Figure 14: $E(t)$ versus t (linear-log scale) for $\epsilon = 0.0$ and 0.1. $N = 1024$, $T = 0.2$. The lines are for the best power fits.

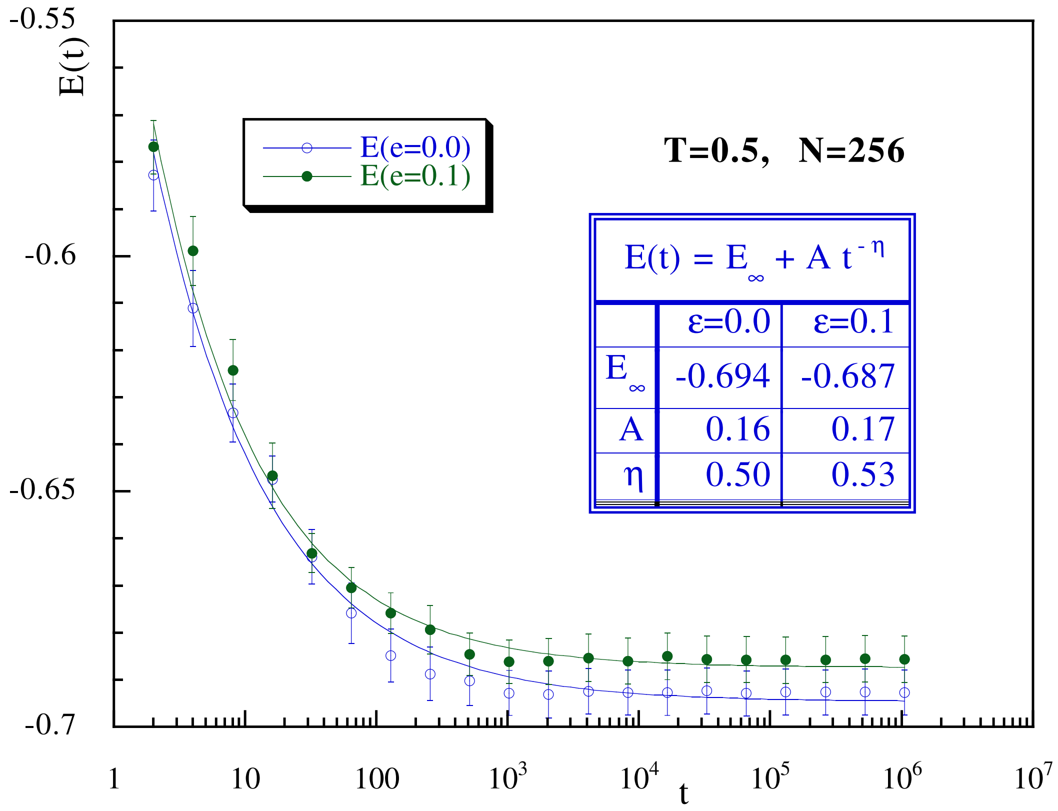

Figure 15: $E(t)$ versus t (linear-log scale) for $\epsilon = 0.0$ and 0.1. $N = 256$, $T = 0.5$. The lines are for the best power fits.

For zero and small ϵ we only see the very slow growth of $q^2(t)$, that is very far from its asymptotic value. At $\epsilon = 0.0$ and $\epsilon = 0.1$ the slow growth is compatible with a logarithmic behavior. For higher ϵ values one starts to see $q^2(t)$ approaching an asymptotic value, but in this case, even when the asymptotic value is very clear, a power fit does not work well. It is interesting to notice that somehow the functional form of the time dependence of $q^2(t)$ is very different from the one of the energy $E(t)$, where the power law is very clear. As we will also show for $T = 0.5$ with fig. (16) the best way to describe the behavior of $q^2(t)$ would be by a very slow logarithmic growth that stops abruptly after reaching its finite volume asymptotic value.

We have also studied the system at higher $T = 0.5$ and smaller volume $N = 256$, by running longer simulations (10^6 steps, and 10 samples for each ϵ value). That has been done in order to reach equilibrium at $\epsilon = 0.0$ and compare with finite ϵ (to check, for example, if the finite ϵ system converges to an effective stable Boltzmann-like probability distribution, see (6). The situation is very similar to the case of $T = 0.2$, with the difference that here the energy and the q^2 plateau's are very clear already at $\epsilon = 0.0$ (equilibrium for both energy and q^2

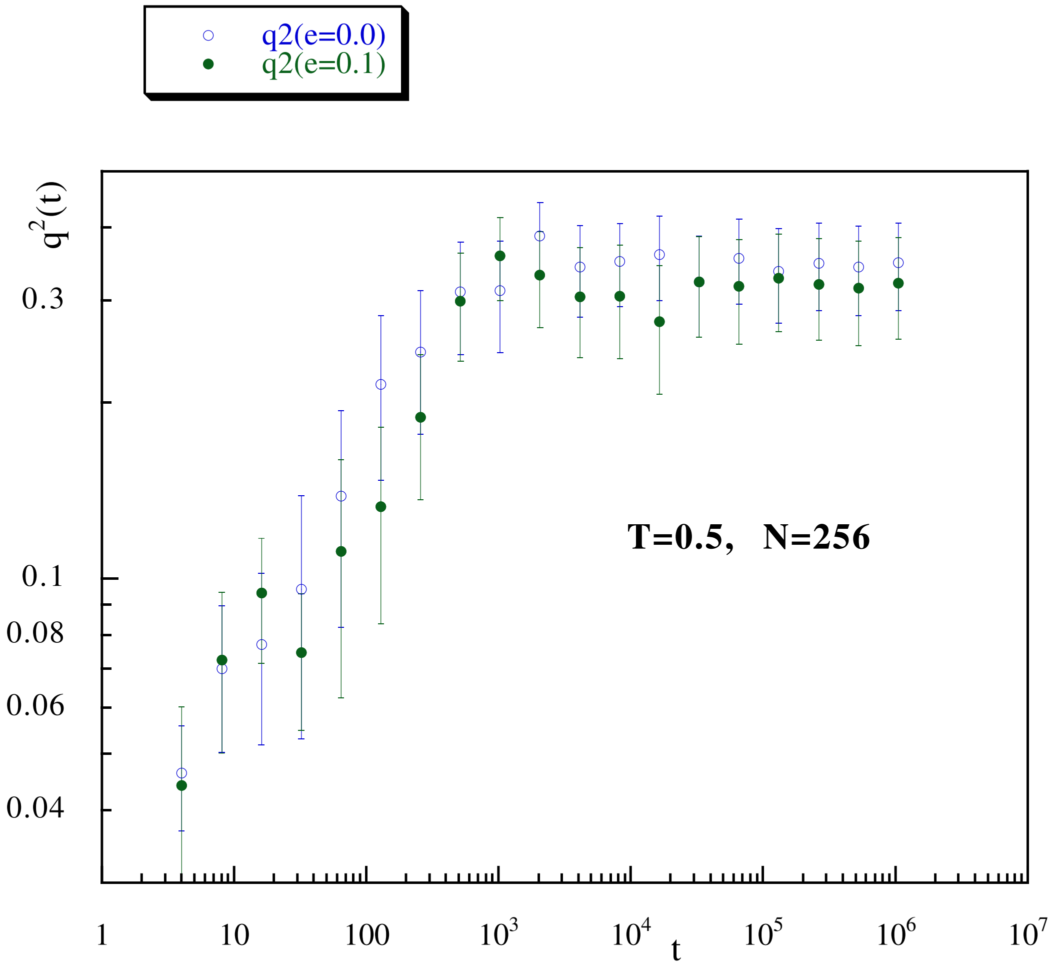

Figure 16: $q^2(t)$ versus t (linear-log scale) for $\epsilon = 0.0$ and 0.1. $N = 256$, $T = 0.5$.

are apparently reached after $O(10^3)$ steps), and the exponents of the power decay are higher (since we are at higher T). We show in fig. (15) $E(t)$ at $\epsilon = 0.0$ and 0.1 with the best power fit (errors are up to $O(5)$ on the last digit). Again the results are very similar, and the power fit is very good. An exponential fit is not able to describe the data. Here already at $\epsilon = .2$ convergence to equilibrium is very fast and an exponential fit works reasonably. At $\epsilon = 0.4$ the best exponent of the power fit is close to one. At $\epsilon = 0.5$ the exponential fit is perfect.

$q^2(t)$ converges to a clear plateau, but as we said it is difficult to find a correct functional form to describe such time dependence. In fig. (16) we show $q^2(t)$ at $\epsilon = 0.0$ and 0.1, where a power fit does not work well. The situation is qualitatively very similar at higher ϵ values, but $q^2(t)$ reaches lower plateau values. At $\epsilon = 0.4$ the asymptotic value of q^2 is very small. At $\epsilon = 0.5$ the asymptotic value of q^2 is 0.02, i.e. fully compatible with zero.

To sum it up, slow convergence to equilibrium is clear for different values of

$T < T_c^{(\epsilon=0.0)}$. We can never see, in the time ranges we investigate, any significant difference when going from $\epsilon = 0.0$ to $\epsilon = 0.1$. It also has to be noticed that in the case where we reach thermal equilibrium for ϵ not too large the expectation value of q^2 at equilibrium is far larger than a pure finite size contamination: for $N = 256$ $\langle q^2 \rangle$ is clearly non zero in a large ϵ range. We will try to understand if this is or not a finite size effect in the next section.

6 Equilibrium

In the former two sections we have analyzed the dynamical properties of the non hamiltonian dynamics. In this section we have taken the complementary point of view and, by studying small lattices on longer time scales we have investigated the equilibrium properties of the model. Even if the model is not defined from an Hamiltonian we can define its equilibrium properties from the large time limit of the dynamics. We have measured the probability distribution of the overlap $P(q)$, and compared the SK model to the non hamiltonian dynamics. We have systematically analyzed the dependence of the equilibrium properties from the finite volume (up to the largest volume on which we have been able to thermalize the system, see later).

We have worked at $T = .5$, running 10^6 full sweeps of the lattice and using the second two thirds of the sweeps for measuring equilibrium properties. We have selected, as before, ϵ going from 0 to 0.5 with increments of 0.1.

We have used $N = 64$, 128 and 256 (respectively with 20, 10 and 10 samples for each ϵ value). In all case we have checked that all the relevant observable quantities (for example $E(t)$, $q^2(t)$) have reached a very clear plateau, where they are stable in all of the measurement region. We have also analyzed directly the sample dependent probability distributions $P_J(q)$ checking the symmetry sample by sample (a very strong check). At $\epsilon = 0$, where the thermalization is more difficult, the $P_J(q)$ is very symmetric at $V = 64$ on all samples. At $V = 128$ there is again a very good symmetry (the maximum discrepancy is of order of 25 per cent of the double peak height. At $V = 256$ some of the samples have a quite asymmetric $P(q)$, but for all 10 systems it looks very plausible that true equilibrium has been reached: the average $P(q)$ is nicely symmetric. We would not have succeeded to thermalize larger systems.

In figures (17)-(18) we plot $P(q)$ for different ϵ and N values (always at $T = 0.5$). It is clear the double peak structure of the Parisi broken phase of the SK model, and that for high ϵ values one gets a trivial distribution centered around $q = 0$.

It is more interesting to follow for example the $\epsilon = 0.3$ case as a function of N. Here from a (already quite soft) double peak structure at $N = 64$ one goes to a broad peak around $q = 0$ at $N = 256$. At $\epsilon = 0.2$ there is the same kind of effect: a strong double peak at $N = 64$ softens at $N = 128$. At $N = 256$ we are

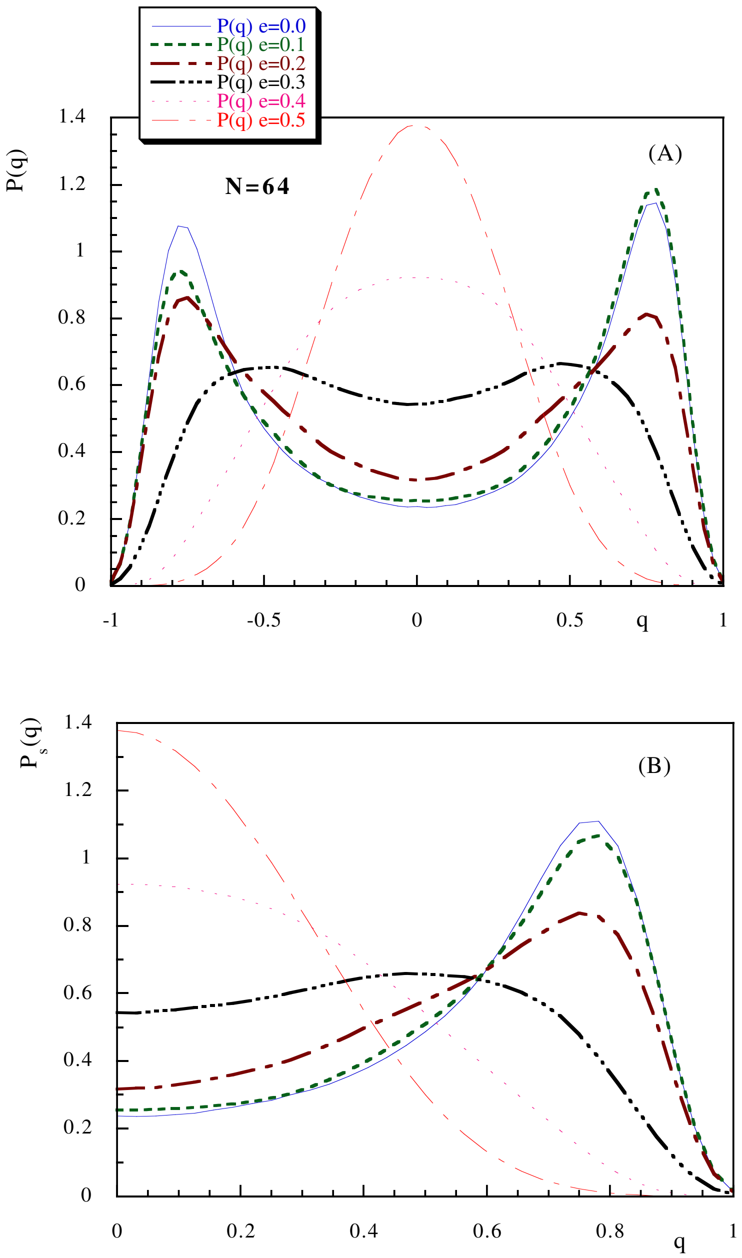

Figure 17: $P(q)$ versus q for different ϵ values, $N = 64$. In (A) the full $P(q)$, where the quality of the symmetry under $q \to -q$ gives a measure of how good our thermalization was. In (B) the symmetrized $P_s(q)$.

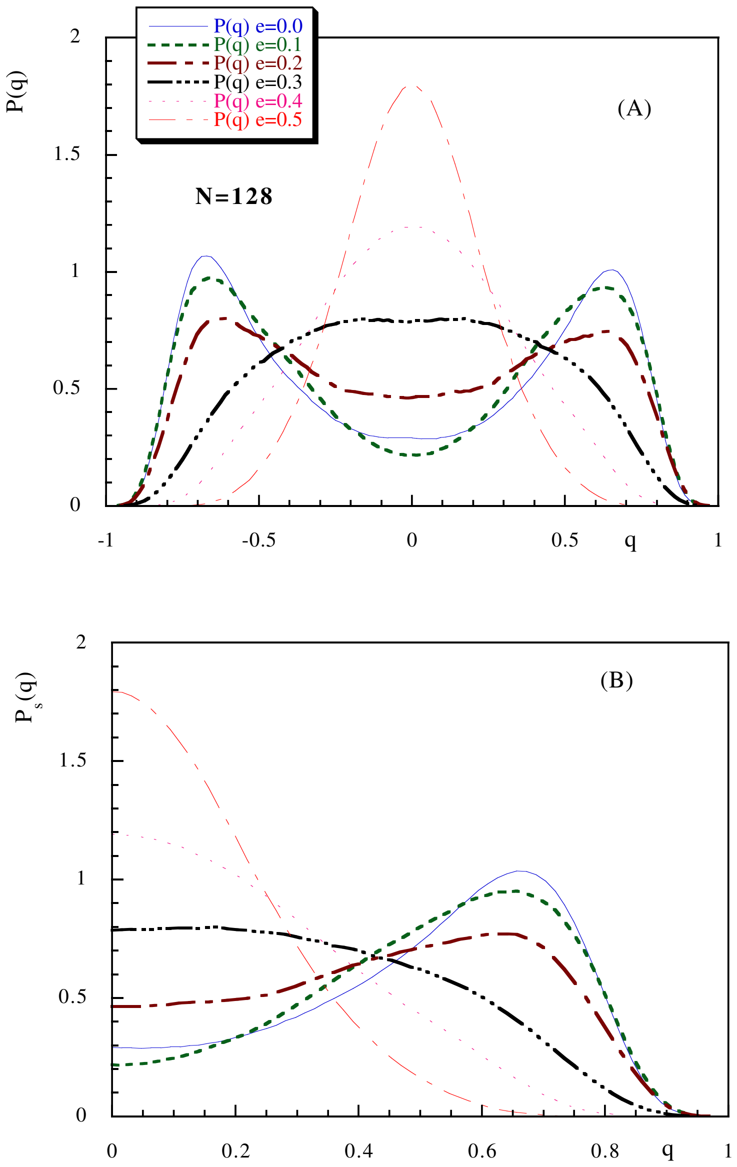

Figure 18: As in figure (17), but $N = 128$.

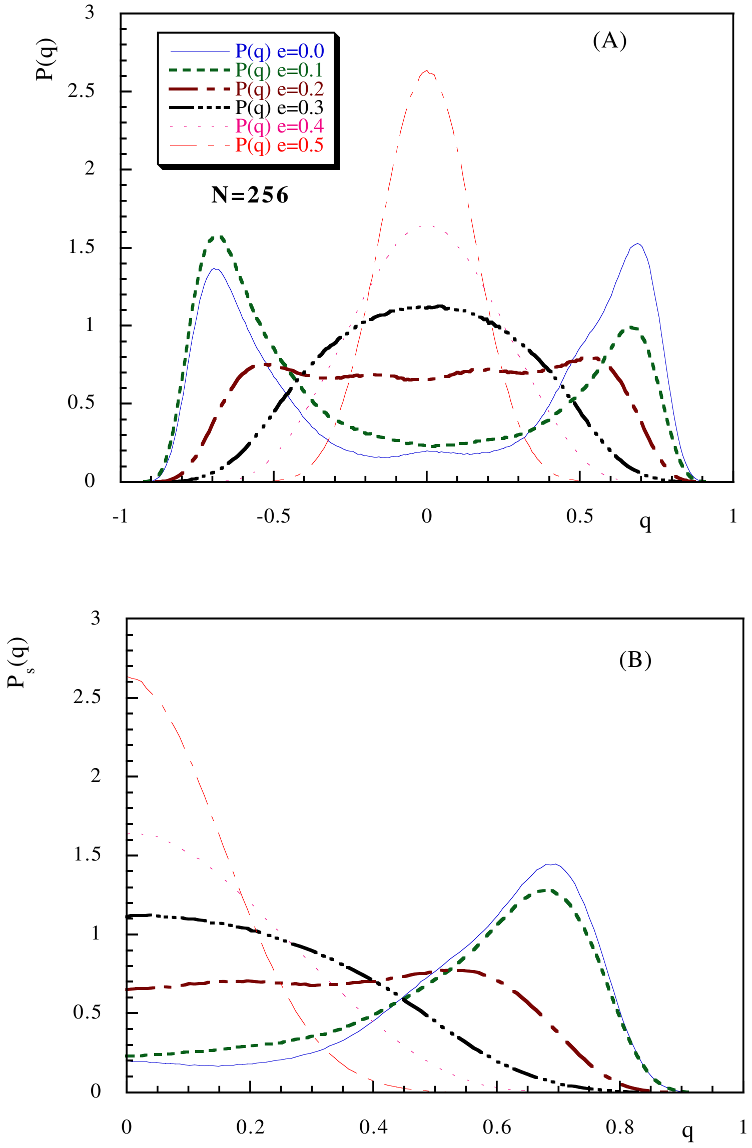

Figure 19: As in figure (17), but $N = 256$.

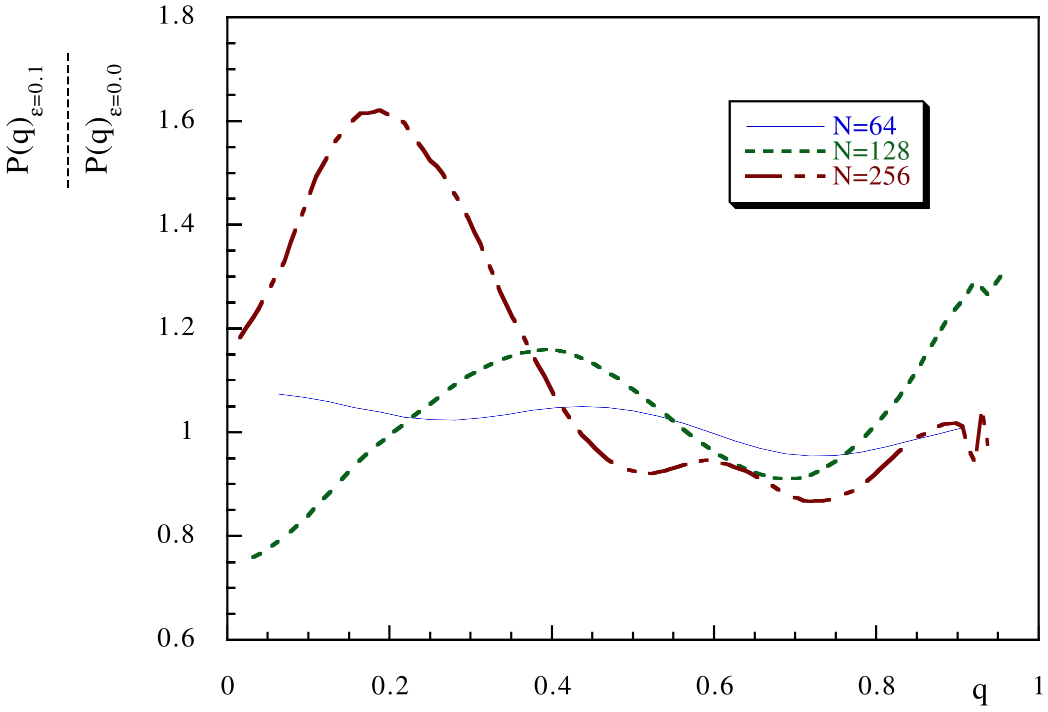

Figure 20: The ratio of $P(q)$ at $\epsilon = 0.0$ and $\epsilon = 0.1$ as a function of q, for different N values.

left with a flat plateau including q values going from $-.5$ to $.5$.

In the case $\epsilon = 0.1$ once again we get results that are very similar to the ones we get for the pure SK model. In our N range we cannot observe any systematic effect.

For making this point more clear we plot in fig. (20) the ratio of the $P(q)$ for the $\epsilon = 0.1$ model and the pure SK model as a function of q, for the three N values we have analyzed. A part from large fluctuations we cannot see any systematic trend. For small q on the large lattice we have a quite large ratio, but the statistical undetermination is in this case large.

In this section we have been exploring features of the model that are different from the dynamical issues we were discussing before. Here we are discussing about equilibrium properties: the system could very well have a complex dynamics on divergent time scales but a trivial large time limit. Still, what we find is that again, on the volume scales we are able to disentangle numerically, there is no difference among the SK model and the one with a small non hamiltonian perturbation. Also we notice that at least for large perturbations the small lattices fake a non-trivial structure, that disappears in the infinite volume limit. The same effect could make trivial the theory with small perturbations on very large volume, but here we cannot see such an effect.

7 Conclusions

Our numerical simulations surely show that the non hamiltonian systems we have studied have a very interesting, complex behavior, and show that the spherical spin model analogy is probably not all of the story.

We have studied aging. We have found that on the time scales we could investigate (that are, one should not forget, of the order of the largest time scales that have been used to claim numerically that the pure model undergoes aging) systems with small perturbations age, while systems with a large non hamiltonian term have a conventional behavior (with some care to be used when discussing the intermediate ϵ case, $\epsilon = 0.2$ for us). Our data do not look compatible with the ϵ^{-6} scaling one finds for the spherical spin model [1, 2]. Also the aging systems look different from the non-aging ones on all time scales, making the possibility of a transient behavior less favored.

We have studied the time dependence of observables like the internal energy $E(t)$ or $q^2(t)$. We have found clear power law decays for small perturbations.

At last we have studied equilibrium. Here we are looking at a regime that is very different from the one discussed before. Also here we have seen that for small perturbations one finds results that are very similar to the ones of the pure model, but we have also seen that for larger ϵ small lattices do produce fake double peak structures in the probability distribution of the overlap.

There is space, as many times is the case, for more analytical and numerical work.

Acknowledgments

We warmly thank David Dean and Daniel Stariolo for many useful exchanges about the subject. We are indebted to Leticia Cugliandolo and Jorge Kurchan for informing us about the results of ref. [12] prior to publication, and for a very explicative and helpful conversation. We acknowledge useful conversations with Giorgio Parisi, Paola Ranieri and Juan Ruiz-Lorenzo.

References

[1] A. Crisanti and H. Sompolinsky, *Dynamics of Spin Systems with Randomly Asymmetric Bonds: Langevin Dynamics and a Spherical Model*, Phys. Rev. **A36** (1987) 4922.

[2] A. Crisanti and H. Sompolinsky, *Dynamics of Spin Systems with Randomly Asymmetric Bonds: Ising Spins and Glauber Dynamics*, Phys. Rev. **A37** (1988) 4865.

[3] J. Hertz, G. Grinstein and S. Solla, in *Neural Networks for Computing,* J. Denker editor, AIP Conference Proceedings **151** (1986) 213.

[4] G. Parisi, *Asymmetric Neural Networks and the Process of Learning,* J. Phys. **A**: (Math. Gen.) **19** (1986) L675.

[5] H. Rieger, M. Schreckenberg and J. Zittartz, *Glauber Dynamics of the Asymmetric SK-Model,* Z. Phys. **B74** (1989) 527.

[6] M. Schreckenberg, *Attractors in the Fully Asymmetric SK-model,* Z. Phys. **B86** (1992) 453.

[7] T. Pfenning, H. Rieger and M. Schreckenberg, *Numerical Investigation of the Asymmetric SK-Model with Deterministic Dynamics,* J. Phys. I **1** (1991) 323.

[8] M. Schreckenberg and H. Rieger, *Remanence Effects in Symmetric and Asymmetric Spin Glass Models,* Z. Phys. **B86** (1992) 443.

[9] H. Eisfeller and M. Opper, *Mean-Field Monte Carlo Approach to the Sherrington-Kirkpatrick Model with Asymmetric Couplings,* Phys. Rev. **E50** (1994) 709.

[10] K. Nützel and U. Krey, *Subtle Dynamic Behavior of Finite-Size SK Spin Glasses with Non-Symmetric Couplings,* J. Phys. **A**: (Math. Gen.) **26** (1993) L591.

[11] R. M. C. de Almeida, L. Bernardi and I. A. Campbell, *Damage Spreading in $\pm J$ Asymmetric Ising Spin Glasses,* J. Phys. I France **5** (1995) 355.

[12] L. F. Cugliandolo, J. Kurchan, P. Le Doussal and L. Peliti, *Glassy Behavior in Disordered Systems with Non-Relaxational Dynamics,* cond-mat/9606060 (June 1996).

[13] H. Sompolinsky and A. Zippelius, Phys. Rev. **B25** (1982) 6860.

[14] L. F. Cugliandolo and J. Kurchan, Phys. Rev. Lett. **71** (1993) 173.

[15] For a recent review see H. Rieger, *Monte Carlo Studies of Ising Spin Glasses and Random Field Systems,* in *Annual Reviews of Computational Physics,* edited by D. Stauffer (World Scientific, Singapore 1995).

[16] L. Cugliandolo, J. Kurchan and F. Ritort, *Evidence of Aging in Spin Glass Mean-FIeld Models,* Phys. Rev. **B49** (1994) 6331.

[17] M. Mezard, G. Parisi and M. Virasoro, Spin Glass Theory and Beyond (World Scientific, Singapore 1987).

[18] G. Parisi, F. Ricci Tersenghi and J. Ruiz-Lorenzo, *Equilibrium and Off-Equilibrium Simulations of the* 4*d Gaussian Spin Glass,* cond-mat/9606051 (July 1996).

[19] D. Rossetti, *Comportamento Dinamico del Modello di Campo Medio dei Vetri di Spin*, *Tesi di Laurea* Università di Roma *La Sapienza* (1995), unpublished.

[20] E. Gardner, B. Derrida and P. Mottishaw, J. Phys. (France) **48** (1987) 741.

[21] H. Eisfeller and M. Opper, Phys. Rev. Lett. **68** (1992) 2094;

[22] G. Ferraro, cond-mat/9407091.

[23] A. Baldassarri, *Non-Equilibrium Monte Carlo Dynamics of the Sherrington-Kirkpatrick Mean Field Spin Glass Model,* cond-mat/9607162 (July 1996).

[24] C. Baillie, D. Johnston, E. Marinari and C. Naitza, *Dynamic Behavior of Spin Glass Systems on Quenched* ϕ^3 *Graphs,* cond-mat/9606194, to be published on J. Phys. **A** (Math. Gen.).